Inference of Reaction Kinetics for Supercritical Water Heavy Oil Upgrading with a Two-phase Stirred Reactor Model

Journal:	*AIChE Journal*
Manuscript ID	AIChE-21-23558
Wiley - Manuscript type:	Research Article
Date Submitted by the Author:	02-Mar-2021
Complete List of Authors:	Raghavan, Ashwin; Massachusetts Institute of Technology, Mechanical Engineering He, Ping; Lamar University, Mechanical Engineering Ghoniem, Ahmed; Massachusetts Institute of Technology, Mechanical Engineering
Keywords:	heavy oil upgrading, supercritical water, Reaction kinetics, two-phase reactor model, coke formation

Inference of Reaction Kinetics for Supercritical Water Heavy Oil Upgrading with a Two-phase Stirred Reactor Model

Ashwin Raghavan*[1], Ping He[2], and Ahmed F. Ghoniem[1]

[1]Department of Mechanical Engineering, Massachusetts Institute of Technology, Cambridge, MA, 02139, USA

[2]Department of Mechanical Engineering, Lamar University, Beaumont, TX, 77710, USA

Abstract

We present the development and application of a two-phase stirred reactor model for heavy oil upgrading in the presence of supercritical water (SCW), with coupled phase-specific thermolysis reaction kinetics and multicomponent hydrocarbon water phase equilibrium. We demonstrate the inference of oil and water phase kinetics parameters for a compact lumped reaction kinetics model through the application of this model to two different sets of batch reactor experiments reported in the literature. We infer that, though SCW can suppress the formation of newer polynuclear aromatics (PNA) from distillate range species, it is broadly ineffective in deterring the combination of pre-existing PNA fragments in the oil feed. Quantification of the conversion to distillate liquids before the onset of coke formation helps arrive at a clearer conclusion on whether the use of SCW in the batch reactor leads to better product outcomes for different oil feeds and operating conditions.

Keywords: heavy oil upgrading, vacuum residue, supercritical water, reaction kinetics, two-phase reactor model, coke formation.

1 Introduction

Supercritical water (SCW), that is, water above it's critical point (T = 374°C, P = 22.1 MPa) is known to be an excellent solvent for low to medium-range boiling point hydrocarbons [1],[2]. Based on this consideration and the hypothesis that SCW could possibly donate hydrogen atoms to smaller polynuclear aromatic (PNA) radicals, thereby, resulting in coking suppression, heavy oil upgrading in the presence of SCW was thought to be a potential technological breakthrough. Over the past two decades, a number of experiments have been performed in batch reactors to study the upgrading of various heavy oils and crude oil vacuum residua (VR) through both, pyrolysis mainly in the oil phase and reaction in the presence of supercritical water ([3]-[8]). A comprehensive summary of these studies may be found in the review by Li et al. [9]. These works consistently conclude that SCW does not have a significant role to play as a participating reactant in the thermolytic processing of heavy oils. However, they suggest different and at times, contradicting effects of the presence of SCW in the reactor on the outcome of the thermolytic process. Though SCW does not participate in the free radical reactions occurring at typical processing temperatures (380°C to 450°C) and pressures (230 to 300 bar), it can affect the rates of various primary cracking and secondary combination reactions by altering the reaction medium. In addition, there exist two phases, a heavy oil-rich phase and a water-rich phase with varying amounts of lighter oil fractions in the water-rich phase depending upon the particular reaction conditions (pressure, temperature and total water to oil mass ratio) governed by thermodynamic phase equilibrium criteria as demonstrated in view-cell experiments by Vilcaez et al. [7] and Kishita et al. [10],[11]. The effect of partitioning or fractionation of the reacting oil species because of the phase split and the potentially different rates of the reactions undergone by the species in each phase has been qualitatively acknowledged in past works ([3]-[8]). However, models coupling the reaction kinetics and multicomponent phase equilibrium that can quantitatively capture these effects have been lacking.

Furthermore, the differences and limitations in the reactant and product oil fractions

quantified in different experiments have led to a lack of clarity on the central question, namely, whether thermolytic processing of heavy oils and vacuum residua in the presence of SCW is indeed significantly beneficial as opposed to pure oil phase pyrolysis. For instance, in the series of batch reactor experiments performed in Shanghai [3],[4], the maltene fraction was not separated into distillate and vacuum residue. As a result, though simple scrutiny of the product data from these batch reactor experiments seems to indicate faster reaction rates in the presence of SCW, one is unable to quantify the important performance metric of conversion to high-value distillate liquids before the onset of coke formation. On the other hand, the series of Japanese batch reactor experiments on whole Athabasca oil sands bitumen (with significant heavy gas oils content in the starting feed) [5],[6] provide product data quantification for the distillate and vacuum residue fractions. However, the lack of sufficient time resolution of the data makes the determination of the coke induction period difficult. As a result, even for these experiments the important performance metric of conversion to high-value distillate liquids before the onset of coke formation can't be easily quantified. Although these experiments indicate lower coke formation for SCW upgrading of the bitumen at longer reaction times, the coke precursor pathway that is being suppressed in the SCW phase is not understood well. Recently, Gudiyella et al. [12] performed detailed GC x GC quantification of lighter hydrocarbon products from the SCW upgrading of Arabian Heavy atmospheric residue. However, comparative experiments for conventional oil phase pyrolysis were not done in that study [12]. Due to the above-mentioned gaps in information and understanding in this field, there is a need for modeling and simulation tools to investigate the SCW upgrading process to throw more light on the batch reactor experiments and their implications in terms of the potential benefits of SCW upgrading.

In this work, we have made an attempt to develop such a numerical simulation tool capable of capturing the effect of the important physical phenomena at play in the supercritical water upgrading of heavy oil. We will describe in detail, the development of a reduced fidelity Two-phase Stirred Reactor (TPSR) modeling tool with (i) chemical reactions in both

phases, (ii) multi-component oil-water phase equilibrium based on detailed thermodynamic modeling suitable for non-ideal mixtures of SCW and heavy oil fractions, products and intermediates, and (iii) a simplified treatment of the interphase species mass transfer rate using an empirical input parameter, the correct value of which, may be determined using high-fidelity CFD simulations of the two-phase flow and mixing process.

The successful application of the TPSR modeling tool to the upgrading of heavy oils and VR in the presence of SCW relies on the formulation and development of an appropriate reaction kinetics sub-model and the inference of the parameter values for the same. It is desirable that such a reaction kinetics model be compact and simple enough to enable parameter inference from existing limited experimental data and at the same time, detailed enough to capture the main features of heavy oil thermolysis. The lumped reaction kinetics model for vacuum residue thermolysis developed by Wiehe [13],[14] strikes a good balance between compactness, simplicity and phenomenological correctness. This model (schematically illustrated in Fig. 3a) correctly encapsulates the following important features of the thermolytic vacuum residue upgrading process:

- **Primary cracking of the maltenic and asphaltenic fractions in the vacuum residue feed** to lower molecular weight maltenic species with decreased aromaticity (referred to as distillate maltenes, MA_d) on the one hand, and maltenic and asphaltenic fractions with increased aromaticity on the other (referred to as maltene cores, MA^+ and asphaltene cores, AS^+ respectively). These chemical pathways can be intuitively thought of as the breaking off of aliphatic side chains from aromatic moieties or fragments in the heavy hydrocarbon fraction molecules as illustrated in Fig. 1. Ample evidence for the dominance of such reactions in the thermolytic upgrading process can be found in experimental studies of both model hydrocarbon compounds [15] and crude oil fractions [12].
- **Initial accumulation of the highly aromatic asphaltene cores in the oil phase**, stabilized in solution by the heavy maltenic fractions and prevented from forming higher molecular weight asphaltene cores by hydrogen donation from the heavy maltenic species

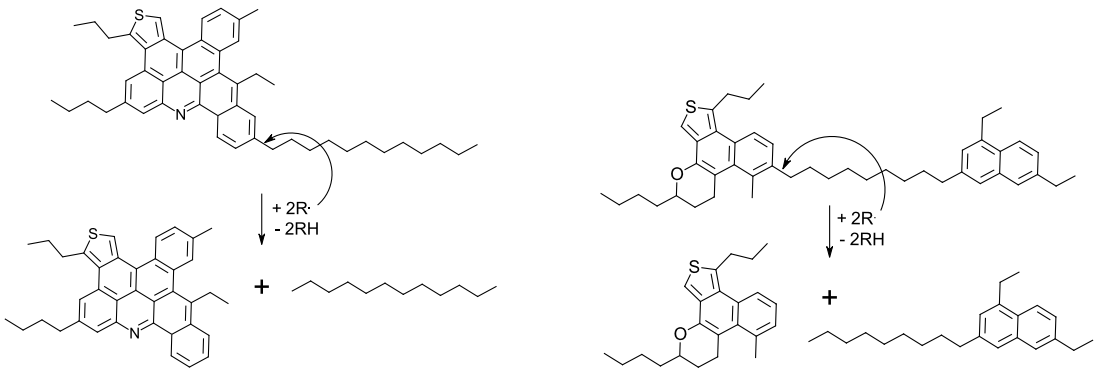

(a) (b)

Figure 1: Primary thermal cracking reaction of a representative (a) asphaltene molecule resulting in a straight chain alkane and lower molecular weight asphaltene with increased aromaticity, and (b) resin maltene molecule resulting in a substituted 2-ring aromatic and lower molecular weight resin with increased aromaticity.

which inhibits the combination reaction pathways.

- **Phase separation of asphaltene cores** triggered once the concentration of AS^{+} in the oil phase exceeds a specific solubility limit, followed by rapid molecular weight growth of the asphaltene cores in the new phase lean in hydrogen donating and dispersing heavy maltenic solvent molecules, **resulting in the formation of solid coke precipitate in the reactor**, as illustrated in Fig. 2.

Owing to the above features, the Wiehe lumped reaction kinetics model [13],[14] is able to capture important characteristics of the batch reactor experimental data for vacuum residue and heavy oil thermolysis like: (i) the coke induction period (wherein no solid coke precipitate is observed in the reactor until a specific reaction time instant) observed in both, Wiehe's extensive experimental work [13],[14] as also in other earlier experimental studies reported in the literature [16]-[23], and (ii) the maximum in asphaltene concentration in the reactor at the onset of coke formation. In fact, the hypothesis of coke formation triggered by phase separation was first postulated by Magaril et al. [18],[24],[25] and was employed in earlier LR kinetic models for VR hydroconversion by Sosnowski et al. [26] and Takatsuka et al. [27]. A detailed discussion of the important chemical pathways and characteristic features of the thermolysis of heavy oils and vacuum residua is taken up in Section 2 of the Supplementary Material. The details of the Wiehe model are elaborated in Section 2.2.1.

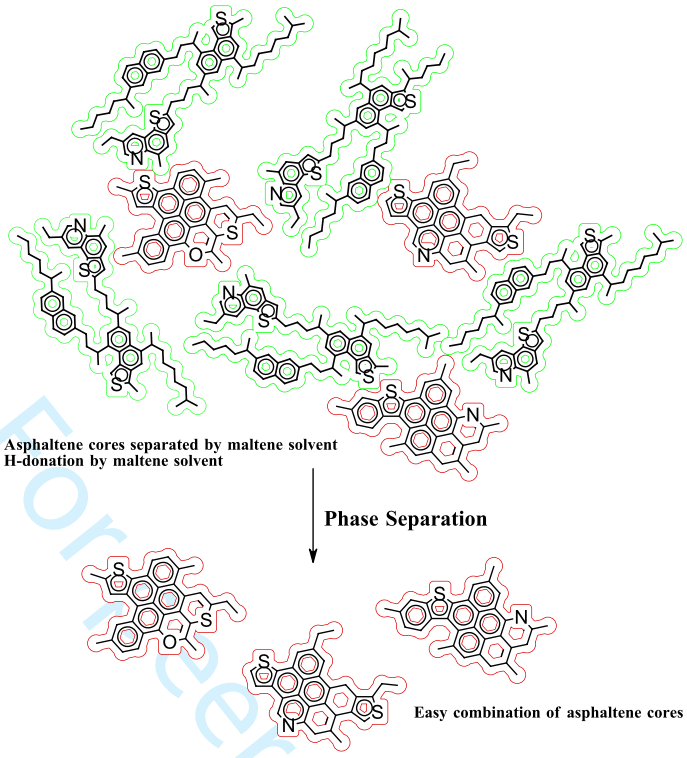

Figure 2: Phase separation of asphaltene cores: (top) In the heavy oil liquid phase, the asphaltene core molecules (red) are separated by heavy aromatic maltene solvent molecules (green) preventing their rapid combination. The combination of asphaltene cores is further retarded by H-donation from the maltenes leading to termination of chain radical pathways (bottom) Once the asphaltene cores form a separate phase, the lack of H-donating and dispersing maltene solvent molecules leads to rapid combination forming solid coke

In recent times, LR kinetics models for heavy oil upgrading in the presence of supercritical water have been proposed by Tan et al. [3] and Liu et al. [4] (schematically illustrated in Fig. 4b), and Li et al. [28] (schematically illustrated in Fig. 4a), in order to fit the batch reactor experimental data in their respective studies. While these models are useful as empirical correlations, they miss out the important phenomenological features of the heavy oil upgrading process discussed above. Moreover, these models do not differentiate between the heavy maltenic species in the original VR feed and the lower molecular weight maltenic species formed through primary cracking. Thus these models are unable to provide a quantitative measure of the success of the upgrading process. In addition, as mentioned earlier, these models assume that the entirety of the reactions in the presence of SCW occur

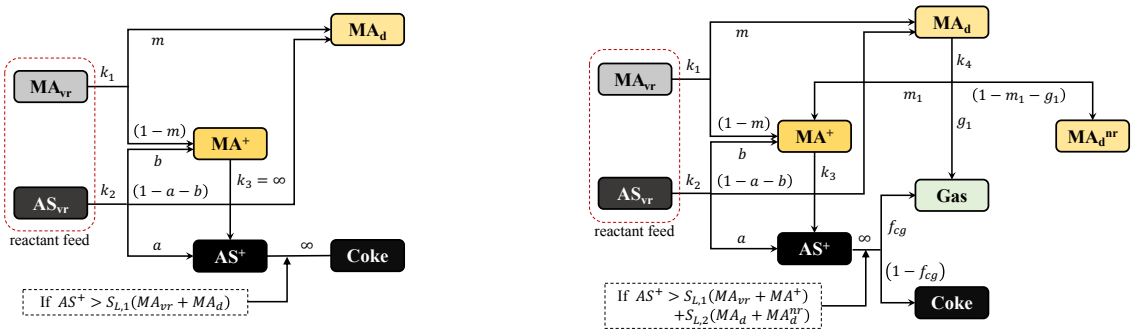

(a) LR model by Wiehe [14],[13] (b) LR model proposed in this work

Figure 3: Schematic of the lumped reaction (LR) kinetics models developed (a) by Wiehe [14],[13], and (b) in this study. **Nomenclature**: MA_{vr}: VR feed unreacted maltenes (heptane-soluble oil fraction), AS_{vr}: VR feed unreacted asphaltenes (heptane-insoluble toluene-soluble oil fraction), MA^{+}: smaller ($\sim$ 2-5 ring) polynuclear aromatics (PNA) or maltene cores, AS^{+}: larger PNAs ($\sim$ 6+ rings) or asphaltene cores, MA_d: high-value distillate maltenes, ${MA_d}^{nr}$: low-reactivity distillate maltenes, S_L: asphaltene cores solubility limit. The k_i marked on the reaction lines originating from each reactant represent the rate constant for that reaction, while the symbols on the split lines connecting to each product represent the stoichiometric co-efficient for that product in the reaction.

in a single phase. As a result, the rate constants determined in their studies may only be taken to be empirical parameters describing the gross chemical transformations between solubility fractions within the whole reactor in the presence of SCW, and not a particular representation of the rate at which these reactions occur within the SCW phase itself.

(a) LR model of Li et al. [28] (b) LR model of Tan, Liu et al. [3],[4]

Figure 4: Schematic of the lumped reaction (LR) kinetics models proposed by (a) Li et al. [28], and (b) Tan, Liu et al. [3],[4]. **Nomenclature**: MA: total maltenes (heptane-soluble oil fraction), AS: total asphaltenes (heptane-insoluble toluene-soluble oil fraction)

In our work, we have developed a compact lumped reaction (LR) kinetics scheme (schematically illustrated in Fig. 3b) for heavy oil upgrading in the presence of SCW building upon

the original LR model for heavy oil thermolysis proposed by Wiehe [13],[14]. The additions and modifications to the Wiehe model done in our work are detailed in Section 2.2.2 and may be briefly summarized as follows:

- A finite rate for the combination reaction of maltene cores (MA^+) towards asphaltene cores (AS^+), so as to develop a reaction model that may be used to investigate the effect of removal of MA^+ from the reactor; for instance, through dissolution into an extractive SCW stream (an investigation of this effect will be discussed in a future study).
- Lumped reaction for secondary retrograde reaction pathway undergone by distillate maltene product, which is important to capture the degradation of the high-value distillate liquid product especially at longer reaction times.
- Separate solubility limit co-efficients for asphaltene cores in distillate and VR maltenes to account for the vastly different ability of these maltenic fractions to hold the AS^+ in solution.
- Formation of gas concurrent with solid coke formation which is dictated by H-balance considerations and appears to be important in order to fit the experimental data closely.
- An analogous set of lumped reactions for the SCW phase governed by different reaction parameters.

We then apply the TPSR model with this LR kinetics scheme to a batch reactor configuration to infer the phase-specific lumped reaction kinetics parameters that best fit the data from two different sets of batch reactor experiments reported in the literature: (i) the Shanghai VR thermolysis experiments [3],[4] and (ii) the Japanese heavy oil bitumen thermolysis experiments [5],[6]. Analysis of the inferred kinetics parameters reveals crucial insights into the effect of the SCW phase environment on primary cracking and coke precursor formation pathways. Specifically, we are able to identify the secondary coke precursor formation pathway from product distillates as the one that is suppressed in the SCW phase, while the primary coke precursor formation pathway from smaller polynuclear aromatic fragments native to the oil feed proceeds at faster rates. In addition, we have quantified the important

performance metric of conversion to high-value distillate liquids before the onset of coke formation for the batch reactor experimental runs reported in the literature [3]-[6] by leveraging the detailed information obtained from the TPSR model simulations. Thus we are able to provide clarity on the fundamental question in the area of heavy oil upgrading, namely under what operating conditions and for which type of of oil feeds does SCW upgrading in batch or co-flow reactors significantly outperform conventional oil-phase thermolysis. Furthermore, the fact that the inferred LR rate constants follow an Arrhenius variation with T can be further exploited in future studies to evaluate the performance of the upgrading process for a wider range of reaction temperatures than those reported in the batch reactor experiments for the same feed.

This paper begins with a detailed discussion of the formulation of the two-phase stirred reactor (TPSR) model and the sub-models involved in Section 2, sub-divided into three main parts (i) the governing equations and numerical solution approach in Section 2.1, (ii) the lumped reaction kinetics scheme in Section 2.2, with a detailed discussion of the major chemical pathways of importance in heavy oil upgrading provided in Section 2 of the Supplementary Material, and (iii) a short summary of the interphase species mass transfer model in Section 2.3, with a detailed discussion of the multi-component phase equilibrium calculation and the required systematic pseudocomponent based thermodynamic modeling procedure for SCW-heavy oil mixtures provided in Section 3 of the Supplementary Material. Thereafter, in Section 3.1, the TPSR model is applied to simulate a series of vacuum residue (VR) upgrading batch reactor experiments performed in Shanghai [3],[4]; to infer the lumped reaction parameters (rate constants and stoichiometric coefficients) for both, the oil phase (in Section 3.1.1) and the SCW phase (in Section 3.1.2). This is accompanied with a detailed analysis of the inferred rate parameters leading to valuable insights into the effect of the SCW phase environment on the major heavy oil upgrading chemical pathways. Furthermore, we demonstrate in Section 3.2 that the TPSR modeling tool with the same form of the LR kinetics model proposed in this study can be employed to infer the reaction parameters for a

different set of reported heavy oil (bitumen) upgrading batch reactor experiments performed in Japan [5],[6]. The inferred phase-specific reaction parameters for these experiments are then analyzed and contrasted with those for the Shanghai experiments in Section 3.2.1, along with an explanation for the major differences. The paper concludes with a discussion of the important performance metric, namely the conversion to high-value distillate liquids before the onset of coke formation, for both, the Shanghai and Japanese experiments in Section 4, which was computed using the detailed information obtained from the TPSR simulations. This reveals the reaction conditions at which heavy oil upgrading in the presence of SCW yields better outcomes than simple pyrolysis for the different oil feeds employed in those studies.

2 The TPSR Model: Formulation and Sub-models

This section details the formulation and development of the Two-phase Stirred Reactor (TPSR) model coupling a detailed numerical treatment of the phenomena of (i) chemical reactions in both phases and (ii) multicomponent phase equilibrium governed by thermodynamics. This is coupled with a simplified treatment of the rate of the two-phase mixing process in terms of a rate towards phase equilibration of the oil-water two-phase system within the reactor.

2.1 Formulation and governing equations

The TPSR model, schematically illustrated in Fig. 5, in essence, tracks the time evolution of each species in each of the two-phases in the reactor. This is done through the numerical solution of the governing equations described below.

1. Species mass conservation for oil phase

$$\frac{d}{dt}\left(m_{o,i}\right) = \underbrace{\dot{m}_{o,in}Y_{o,i,in}}_{(\mathbb{I})} - \underbrace{\dot{m}_{o,out}Y_{o,i}}_{(\mathbb{O})} - \underbrace{\dot{m}_{o\rightarrow w,i}}_{(\mathbb{S}_\Sigma)} + \underbrace{\dot{\omega}_{o,i}}_{(\mathbb{S}_R)} \qquad \forall\, i = 1, 2, ..., N_{sp} \tag{1}$$

2. Species mass conservation for water phase

$$\frac{d}{dt}\left(m_{w,i}\right) = \underbrace{\dot{m}_{w,in}Y_{w,i,in}}_{(\mathbb{I})} - \underbrace{\dot{m}_{w,out}Y_{w,i}}_{(\mathbb{O})} + \underbrace{\dot{m}_{o\rightarrow w,i}}_{(\mathbb{S}_\Sigma)} + \underbrace{\dot{\omega}_{w,i}}_{(\mathbb{S}_R)} \qquad \forall\, i = 1, 2, ..., N_{sp} \tag{2}$$

3. Total reactor volume constraint

$$\frac{\sum_{i=1}^{N_{sp}} m_{o,i}}{\rho_o} + \frac{\sum_{i=1}^{N_{sp}} m_{w,i}}{\rho_w} = V_{r,0} \tag{3}$$

In Eq. (1) to Eq. (3) above, the sub-scripts "o" and "w" refer to the oil phase and water phase respectively. Thus, $m_{o,i}$ and $m_{w,i}$ are the masses of species i in the oil phase and water phase respectively with $Y_{o,i}$ and $Y_{w,i}$ being the corresponding spatially-averaged species mass-fractions; ρ_o and ρ_w are the phase densities, while $V_{r,0}$ is the total reactor volume, which is to be maintained constant throughout the simulation. The terms ($\mathbb{I}$) and ($\mathbb{O}$) in Eq. (1) and Eq. (2) represent the species mass flow into and out of the reactor respectively. Here, the compositions of the inflow streams corresponding to each phase $Y_{o,i,in}$ and $Y_{w,i,in}$ are assumed to be known constants. The compositions of the outflow streams are assumed to be equal to the bulk compositions of the respective phases, that is, the inhomogeneity within each phase has been neglected. For the problem to be well-posed, in the absence of any other constraints, only one among the mass-flow rate variables ($\dot{m}_{o,in}$, $\dot{m}_{w,in}$, $\dot{m}_{o,out}$, $\dot{m}_{w,out}$) may be unknown with the others being specified input conditions. The terms labeled ($\mathbb{S}_R$) in Eq. (1) and Eq. (2) represent the source terms due to chemical reactions. These unclosed terms are calculated using the chemical reactions sub-model based on a lumped reaction kinetics scheme with different kinetics parameters for the oil and water phases, as described in detail in Section 2.2. The terms labeled ($\mathbb{S}_\Sigma$) in Eq. (1) and Eq. (2) represent the source terms due to interphase species mass transfer. These unclosed terms are computed using the interphase species mass transfer sub-model involving detailed multicomponent phase equilibrium calculations along with a simplified empirical treatment of the rate towards phase equilibration, as described in detail in Section 2.3.

The above formulation gives a system of $(5N_{sp}+1)$ equations in $(5N_{sp}+1)$ unknown

variables. Here, the $(5N_{sp}+1)$ unknowns are comprised of (i) $2N_{sp}$ species masses corresponding to the oil and water phases ($m_{o,i}$ and $m_{w,i}$) (ii) One out of the inflow and outflow rates ($\dot{m}_{o,in}$, $\dot{m}_{w,in}$, $\dot{m}_{o,out}$, $\dot{m}_{w,out}$) (iii) $2N_{sp}$ unclosed chemical reaction source terms ($\dot{\omega}_{o,i}$ and $\dot{\omega}_{w,i}$) and (iv) N_{sp} unclosed interphase species mass transfer source terms ($\dot{m}_{o\rightarrow w,i}$). The $(5N_{sp}+1)$ equations are comprised of (i) N_{sp} species conservation equations (Eq. (1)) for the oil phase (ii) N_{sp} species conservation equations (Eq. (2)) for the water phase (iii) One reactor volume constraint (Eq. (3)) (iv) $2N_{sp}$ closure relations for the chemical reaction source terms corresponding to both phases (Section 2.2) and (v) N_{sp} closure relations for the interphase species mass transfer source terms (Section 2.3).

The above system of coupled ODEs and non-linear equations are solved numerically using an algorithm wherein, the ODEs are marched ahead in time using an Euler explicit temporal discretization scheme. The algorithm also involves an iterative solution at each time-step to ensure temporal convergence of the coupled system of equations at each time-step. Typically, 4-5 iterations suffice for the small numerical time-steps adopted in the applications of the TPSR model performed in this work. The numerical implementation was done in *MATLAB* with the linking of *C++* and *Fortran* libraries for the thermodynamic and phase equilibrium calculations. The entire source code can be viewed on the github repository [29].

In this study, the TPSR simulation tool was run in the batch reactor mode to perform the inference of phase-specific reaction kinetics parameters by simulating experiments reported in the literature. The details of the different modes of operation for the TPSR model are explained in Section 1 of the Supplementary Material.

2.2 Chemical reaction sub-model

As heavy crude oils and vacuum residua contain millions of molecules, it is infeasible to track the chemical transformations of each individual molecule through fundamental reactions. Hence, we adopt a lumped reaction modeling approach wherein, large groups of hydrocarbon molecules with similar chemical characteristics are described together using pseudocomponent lumps. Only global reactions affecting net chemical transformations

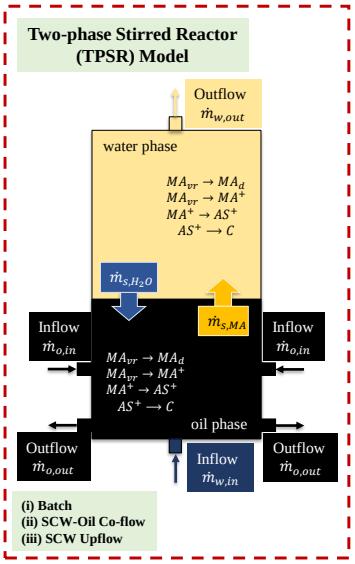

Figure 5: Two-phase Stirred Reactor (TPSR) model schematic

between these lumps are represented. Though this approach may appear to be an over-simplification, it has been shown to be very effective in describing the characteristic features of heavy oil and vacuum residue thermolysis [13],[14]. The success of any such lumped reaction scheme rests upon choosing just enough and the right species lumps and reactions in order to represent the important chemical reaction pathways in the system. The important chemical reaction pathways in the thermolysis of heavy oils and vacuum residua are briefly summarized below to provide context for the formulation of a lumped reaction scheme for the TPSR model. These chemical reaction pathways are discussed in great detail in Section 2 of the Supplementary Material.

- **Primary cracking of heavy hydrocarbon fractions** is the major pathway leading to the "upgrading" of the heavy oil feed and involves breaking off the aliphatic side chains from aromatic moieties or fragments in the heavy hydrocarbon fraction molecules as illustrated in Fig. 1a and Fig. 1b.
- **Combination of aromatic fragments** ($\sim$ 2-5 ring) as illustrated in Fig. 6a, to form large polynuclear aromatics ($\sim$ 6+ rings) which are precursors to coke, is an important pathway leading to undesirable and unnecessary coke formation in upgrading processes.

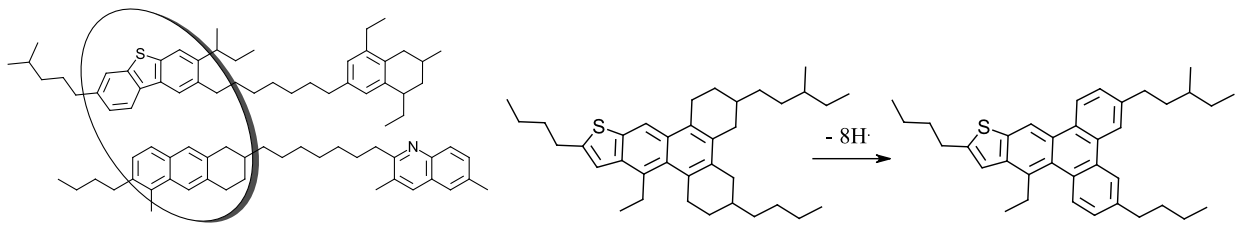

(a) (b)

Figure 6: (a) Combination of smaller 3-ring aromatic fragments to form a large 6-ring polynuclear aromatic fragment similar to the aromatic core structures found in asphaltene molecules, (b) Aromatization of hydroaromatics by dehydrogenation of naphthenic rings adjacent to aromatic rings resulting in the formation of larger polynuclear aromatic molecules.

- **Solid coke formation from large polynuclear aromatics** once the solubility limit of the large PNAs in the liquid phase is exceeded, as illustrated in Fig. 2.
- **Secondary cracking and retrograde reactions** of distillate fractions, involving cyclization to form hydroaromatics followed by their aromatization (illustrated in Fig. 6b), resulting in the formation of smaller aromatic cores and volatile gases.

2.2.1 Lumped reaction kinetics model for vacuum residue thermolysis in oil phase: The base model

The work of Wiehe in [13], [14] provides a good base model representing the important chemical pathways and features of vacuum residue thermolysis described in detail in Section 2 of the Supplementary Material. This lumped reaction scheme (schematically illustrated in Fig. 3a) consists of the following reactions:

1. **Primary cracking of vacuum residue maltenes:**

$$MA_{vr} \xrightarrow{k_1} m\, MA^{+} + (1-m)\, MA_d \quad \ldots (R1) \tag{4}$$

Here, the MA_{vr} species lump represents the VR feed maltenes; MA^{+} represents the smaller PNAs ($\sim$ 2-5 ring aromatics) or maltene cores and MA_d represents the desired high-value distillate liquid product.

2. **Primary cracking of vacuum residue asphaltenes:**

$$AS_{vr} \xrightarrow{k_2} a\, AS^{+} + b\, MA^{+} + (1-a-b)\, MA_d \quad \ldots (R2) \tag{5}$$

Here, the AS_{vr} species lump represents the VR feed asphaltenes and AS^{+} represents the larger PNAs ($\sim$ 6+ ring aromatics) or asphaltene cores.

3. **Combination of maltene cores to asphaltene cores:**

$$MA^{+} \xrightarrow{k_3} AS^{+} \quad ... (R3) \tag{6}$$

4. **Solid coke formation through phase separation of asphaltene cores:**

$$AS^{+}_{ex} \xrightarrow{\infty} C \quad ... (R5) \tag{7}$$

Here, C is the solid coke formed at an infinitely fast rate from the asphaltene cores in excess of the solubility limit (S_L) in the liquid phase ($AS_{ex}{}^{+}$) given by:

$$AS^{+}_{ex} = AS^{+} - S_L(MA_{vr} + MA^{+} + MA_d) \tag{8}$$

Wiehe simplified the above model and reduced the number of kinetics parameters by assuming an infinitely fast rate for reaction (R3) based on the considerations that (i) k_3, like k_2, is likely to be significantly faster than k_1 in the temperature range of their experiments (390°C to 420°C) and (ii) the maltene cores are not removed from the oil phase in the reactor in any way in their experiments, which results in them ultimately forming asphaltene cores. In addition, Wiehe showed that the solubility limit coefficient (S_L) is lower when the product distillates remain in the oil phase in closed-tube reactor experiments as opposed to open-tube rector experiments where they volatilize out of the tube. This is mainly due to the fact that the lighter product distillate fraction is an inferior solvent and H-donor for AS^{+} as compared to the heavy maltene fractions in the VR feed.

2.2.2 An improved lumped reaction kinetics model for heavy oil thermolysis in the presence of SCW

In our work, we further improved upon the Wiehe model [13], [14] discussed in the previous section, leading to the development of an augmented LR model as illustrated schematically in Fig. 3b. The major modifications and additions are as follows:

1. **A finite rate constant k_3 for the maltene core combination reaction (R3):** One of

the planned objectives of the present work is to develop the modeling capability to capture the effects of the removal of MA^+ from the reactor; for instance, through dissolution into an extractive SCW stream (an investigation of this effect will be discussed in a future study). A finite k_3 is essential to capture the effect of such removal of MA^+ from the reactor.

2. **Lumped reaction for secondary retrograde reaction pathway of distillate maltene product:** Wiehe qualitatively acknowledged the importance of the secondary reaction pathway of product distillates towards volatiles (mainly C_1-C_4 gases) and maltene cores, especially at higher T ($> 420°C$) [14]. However, this pathway was not modeled in their work. This reaction pathway leads to a decrease in both the quantity and quality (in terms of H-content) of the high-value distillate liquid product of the upgrading process. In our work, we have modeled this secondary reaction pathway as shown below:

$$MA_d \xrightarrow{k_4} m_1\, MA^+ + g_1\, G + (1 - m_1 - g_1)\, MA_d^{nr} \quad \ldots (R4) \tag{9}$$

Here, G represents the gas fraction while ${MA_d}^{nr}$ represents the low-reactivity distillate species formed from the secondary reaction pathway. In the Shanghai batch reactor experiments [3],[4], it has been consistently observed that at very long reaction times, a pseudo-equilibrium state is established with the total maltene mass fraction approaching a steady-state value. The introduction of a low-reactivity maltene end-product ${MA_d}^{nr}$ into the model was done in order to capture this phenomenon. In the absence of this end-product, the maltene mass fraction would approach zero at long reaction times, which is not the case in reality.

3. **Separate solubility limit coefficients for asphaltene cores in distillate and VR maltenes:** The excess asphaltene cores are determined using the following relation accounting for the difference in the ability of the less aromatic distillate products and more aromatic VR feed maltenes and maltene cores to stabilize the asphaltene cores in the

liquid phase:

$$AS_{ex}^{+} = AS^{+} - S_{L,1}(MA_{vr} + MA^{+}) - S_{L,2}(MA_{d} + MA_{d}^{nr}) \quad (10)$$

4. **Formation of gas concurrent with solid coke formation:** The data from vacuum residue thermolysis batch reactor experiments [3],[4] show that a part of the gas formed is concurrent with solid coke formation. This is observed for both pure oil phase thermolysis as well as reaction in the presence of SCW. Furthermore, the average H-content of solid coke formed is $\sim$ 4 to 5.5 wt%, while that of the coke precursors or AS^{+} is $\sim$ 6.5 wt%. H-balance dictates the formation of gas during the transformation of AS^{+} to solid coke. Hence, reaction (R5) in Eq. (7) was modified as follows:

$$AS_{ex}^{+} \xrightarrow{\infty} f_{cg}\, G + (1 - f_{cg})\, C \quad \ldots (R5) \quad (11)$$

Here, f_{cg} is the "coke gas fraction" or the fraction of gas formed in the final solid coke formation reaction. The nominal value of f_{cg} can be calculated to be $\sim$ 0.1 to 0.2 from an approximate H-balance of Eq. (11) assuming the average H-content values for solid coke, AS^{+} and gas as 4.0-5.5, 6.5 and 20 wt%, respectively.

The same set of lumped reactions also occur in the SCW phase with different rate parameters. Fig. 3b shows a schematic representation of our LR kinetics model. The stoichiometric coefficients m, a and b are the same for the oil and SCW phase reactions. In addition, they do not change with the reaction temperature. These coefficients mainly depend on the aromatic content of VR feed maltenes and asphaltenes. They only change slightly for different VR feeds as shown in [14]. Due to the limited amount of experimental data available to us for kinetics parameter inference, these stoichiometric co-efficients were kept unchanged and equal to those for Cold Lake VR in [14]. The coke gas fraction is also a constant with respect to T and the same for both oil and SCW phase reactions. It is clear from the nature of the above LR scheme involving reaction pathways between pseudocomponent species occurring with different rate parameters in the oil and SCW phases, that the TPSR model

must incorporate the following physical modeling capabilities:

1. Thermodynamic modeling for heavy oil fractions, intermediates and light end products in the form of pseudo-component representations like MA_{vr}, AS_{vr}, MA_d and MA^+
2. Phase equilibrium calculations for systems of these pseudo-components and water, and
3. Modeling the rate of transfer of species from one phase to another with the total possible amount of this transfer being limited by thermodynamic phase equilibrium criteria

These capabilities of the TPSR model are encompassed in the interphase species mass transfer sub-model, discussed in the following section.

2.3 Interphase species mass transfer sub-model

The interphase species mass transfer sub-model for calculating $\dot{m}_{o\rightarrow w,i}$ for each of the species at each time-step of the TPSR model simulation is comprised of two parts as follows:

1. **Multicomponent phase equilibrium consistent with non-ideal thermodynamics of the system of SCW and oil species:** The multicomponent phase equilibrium calculations give the maximum limit for interphase transfer of each species as allowed by thermodynamic considerations. This maximum amount of species transfer may be realized within a given time-step of the simulation only for an infinitely fast two-phase mixing process. The details of the multicomponent phase equilibrium calculation are discussed in Section 3.1 of the Supplementary Material. A robust multicomponent phase equilibrium calculation was implemented within the TPSR simulation tool based on the successive-substitution method. The details of this algorithm may be found in the seminal work of Michelsen [31],[32]. The source code for the numerical implementation may be found in the TPSR model code repository on github [29].
2. **Simple empirical treatment for the rate towards phase equilibrium:** The rate at which the aforementioned interphase species transfer limited by phase equilibrium occurs may be computed using either one of two simplistic models: (i) instantaneous phase equilibration approximation, corresponding to a scenario where the two-phase mixing process occurs over time-scales much shorter than those of the thermolysis chemical

reactions, OR (ii) partial phase equilibration approximation, appropriate for scenarios wherein the two-phase mixing process is only fast enough to allow a fraction of the computed multicomponent phase equilibrium to reach completion within a time-step of the TPSR simulation. In this study, we have employed the instantaneous phase equilibration approximation, which is discussed further in Section 3.2 of the Supplementary Material. The partial phase equilibration model will be employed in a future study to quantify the effect of finite two-phase mixing rates on the upgrading process in flow reactors.

2.4 Thermodynamic modeling

The multi-component phase equilibrium calculation described in the section above requires the calculation of species fugacity co-efficients representative of the non-ideal thermodynamics of hydrocarbon-water multi-component mixtures in the T, P range of interest for the SCW heavy oil upgrading process (T = 380°C to 450°C and P > 230 bar). In this work, we have employed a thermodynamic modeling procedure based on the Predictive Peng-Robinson (PPR78) Cubic Equation of State [38],[39],[40],[41], in conjunction with a systematic pseudo-component modeling procedure to estimate the thermodynamic parameters for the heavy oil feed fractions, products and intermediates. A concise discussion of the thermodynamic model is included in Section 3.3 of the Supplementary Material. A more detailed discussion of this equation of state modeling approach and the computation of thermodynamic quantities from the same may be found in our previous works [33]-[35]. The details of the comprehensive pseudo-component modeling procedure (illustrated schematically in Fig. 4 in the Supplementary Material) may be found in the work of He and Ghoniem [47].

3 Results: Inference of lumped reaction kinetics parameters

Different heavy oil and VR feeds are bound to have significantly different reactivities. Consequently, phase-specific LR kinetics parameters must be inferred for different oil feeds using batch reactor experimental data for the corresponding feed. In this paper, we demonstrate that a systematic parameter inference procedure using the TPSR model may be ap-

plied repeatably to obtain phase-specific LR kinetics parameters for the lumped reactions discussed in Section 2.2.1 and Section 2.2.2, for different heavy oil feeds. The TPSR model was applied to simulate two different sets of batch reactor experiments reported in the literature: (i) the Shanghai VR thermolysis experiments [3],[4], and (ii) the Japanese heavy oil bitumen thermolysis experiments [5],[6]. In these studies, experiments were performed both in the presence of (i) N_2, to mimic predominantly oil phase reaction and (ii) SCW, with reactions occurring in both oil and water phases. The operating conditions for these experiments are shown in Table B1 and Table B2 in the Supplementary Material.

The set of lumped reaction (LR) parameters p_i (i = 1,2,...,9) that need to be inferred from TPSR simulations of the batch reactor experiments are:

1. p_1 to p_4: The reaction rate constants k_1 to k_4 corresponding to the reactions (R1) to (R4).
2. p_5 to p_7: The stoichiometric co-efficients m_1, g_1 and f_{cg}
3. p_8 and p_9: The solubility limit co-efficients $S_{L,1}$ and $S_{L,2}$

The parameters p_{10} to p_{12} corresponding to the stoichiometric co-efficients m, a and b in reactions (R1) and (R2) were assumed to have numerical values of 0.302, 0.602 and 0.108 respectively for all temperatures and reaction media. These values are the same as those reported in Wiehe's work for Cold Lake VR thermolysis in the oil phase [14].

For each of the experimental runs at different reaction temperatures and with different reaction media (N_2 and SCW), TPSR simulations were set up with the initial conditions corresponding to the specified T and reaction medium as shown in Table B1 and Table B2 in the Supplementary Material. Multiple TPSR simulations were performed, varying one LR parameter at a time until a reasonably good fit (mean square error $\sim$ 1e-5 to 1e-4) to the experimental data was obtained. The mean square error for the i^{th} simulation run corresponding to the variation of the LR parameter p_i was defined as:

$$e_{ms,i} = \frac{\sum_{n=1}^{N}\sum_{l=1}^{L}[y_l(t=t_n) - \bar{y}_l(t=t_n)]^2}{(N.L)} \tag{12}$$

Here, y_l $(t = t_n)$ is the mass fraction of the l^{th} species lump measured at the time-instant t_n

in the experiment and $\bar{y}_l$ $(t = t_n)$ is the corresponding value for the TPSR simulation run. L and N refer to the total number of species lumps and total time instants for which data was measured in the respective experiment.

3.1 Shanghai VR thermolysis experiments

The TPSR model was applied to simulate the series of VR thermolysis experiments [3],[4] performed in Shanghai in a 100 mL Parr 4598-HPHT stirred (stirring rate of 800 rpm) autoclave reactor. These works report experimental runs at three different reaction temperatures (390°C, 410°C and 430°C) for thermolysis of a heavy oil vacuum residue feed from Sinopec Shanghai Petrochemical Company containing 95 wt% maltenes and 5 wt% asphaltenes. The operating conditions for these experiments are shown in Table B1 in the Supplementary Material. The total number of species lumps measured in the Shanghai experiments was $L = 4$, namely (i) total maltene (ii) total asphaltene (iii) coke and (iv) gas. The total maltene mass fraction was calculated as the sum of the mass fractions of the species MA_d, $MA_d{}^{nr}$, MA^+, $MA_{vr,l}$ and $MA_{vr,h}$. The total asphaltene mass fraction was calculated as the sum of the mass fractions of the species AS^+ and AS_{vr}.

The pseudo-components (PCs) used for the modeling of the feed oil fractions, products and intermediate species are given in Table 2 in the Supplementary Material, along with their mass fractions in the initial VR feed. The PCs used in this study are based on those developed in a previous work on the pseudo-component modeling of heavy oils and vacuum residua by He and Ghoniem [47]. A detailed discussion of the PCs chosen for this study is included in Section 3.4 of the Supplementary Material.

3.1.1 Best-fit oil phase lumped reaction kinetics parameters

The experimental runs for the VR thermolysis in the presence of N_2 were used to infer the oil phase lumped reaction (LR) parameters. This is a reasonable approach as only the gas and MA_d (to a lesser extent) fractions have significant solubility in the N_2 at the T, P conditions of the experiments. The oil phase parameters resulting in the best fit between the TPSR model predictions and the experimental data [3],[4] are given in Table C1 in the

Supplementary Material, along with the corresponding values for the base model parameters from Wiehe's work [13], [14]. The TPSR model predictions for the temporal variation of the species lump mass fractions for those best-fit kinetic parameters are shown in Fig. 7a to Fig. 7c along with the experimental data [3],[4] points (solid markers), indicating a good fit between the model predictions and the experimental data. In particular, important characteristics of VR thermolysis like the coke induction period and total asphaltene increase up to the onset of coke formation (which can be clearly observed in Fig. 7b and Fig. 7c) are captured correctly. The total asphaltene fraction keeps increasing initially and reaches a maximum at the onset of coke formation due to the accumulation of asphaltene cores (AS^{+}) in the oil phase. Thereafter, the total asphaltene fraction decreases as AS^{+} gets precipitated as coke. The reaction representing the secondary reaction of distillate product also helps to predict correctly the species lump mass fractions at long reaction times approaching the correct pseudo-equilibrium values as in the experiments.

The primary cracking rate constants k_1 and k_2 at 390°C, 410°C and 430°C obtained from the fitting procedure are very close to those found for Cold Lake VR in Wiehe's work [14] as shown in Table C1 in the Supplementary Material. Here, the k_1 and k_2 values at 390°C, 410°C and 430°C for Cold Lake VR were interpolated from the values reported at 370°C, 400°C and 420°C in [14], based on an Arrhenius variation of the rate constants with T.

The value of the AS^{+} solubility limit co-efficient for MA_{vr} and MA^{+} ($S_{L,1}$) was found to be 0.36 at both T = 410°C and 430°C. This value is very close to the solubility limit co-efficient S_L for Cold Lake VR thermolysis at T = 400°C in open-tube reactors reported in Wiehe's work [14]. In open-tube reactors, the distillate product volatilizes out of the tube. As a result, the ability of the VR feed maltenes and maltene cores to hold the AS^{+} in solution mainly determines the AS^{+} solubility limit. In the thermolysis experiments in the presence of N_2, increasingly higher amounts of MA_d dissolve into the N_2 phase at the higher temperatures of T = 410°C and 430°C resulting in the oil phase being leaner in the distillate fraction similar to open-tube experiments. Consequently, the value of $S_{L,1}$ is close

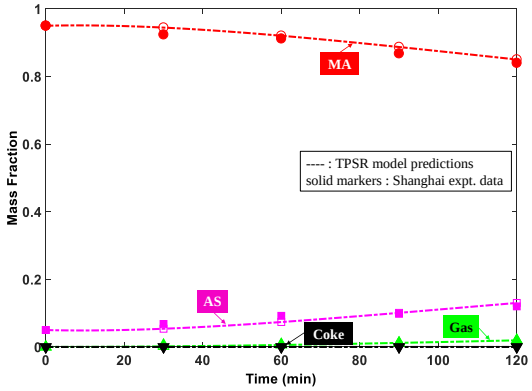

(a) P = 180 bar, T = 390°C

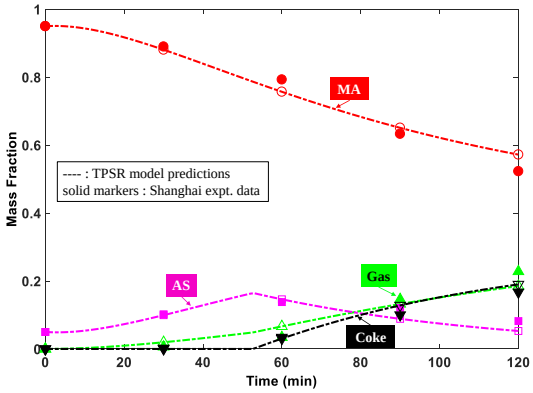

(b) P = 190 bar, T = 410°C

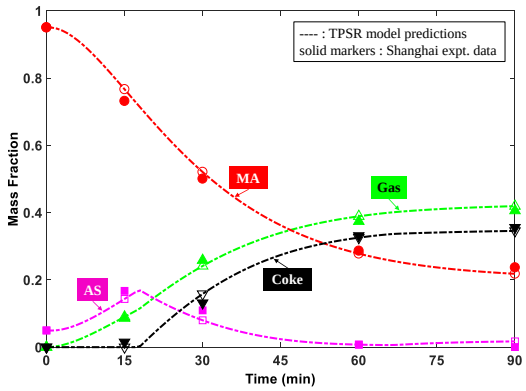

(c) P = 200 bar, T = 430°C

Figure 7: TPSR model predictions of temporal variation of reaction species lumps using the best-fit kinetic parameters for the Shanghai batch reactor experiments ([3],[4]) of VR pyrolysis in the presence of N_2. As seen in (b) and (c), the total asphaltene fraction keeps increasing initially and reaches a maximum at the onset of coke formation due to the accumulation of asphaltene cores (AS^+) in the oil phase. Thereafter, the total asphaltene fraction decreases as AS^+ gets precipitated as coke. Nomenclature: MA: total maltene; AS: total asphaltene.

to the open-tube reactor experiment value for S_L. On the other hand, the value of the AS^+ solubility limit co-efficient for MA_d ($S_{L,2}$) was found to be 0.15 at both T = 410°C and 430°C. This value is very close to the solubility limit co-efficient S_L for Cold Lake VR thermolysis at T = 400°C in closed-tube reactors reported in Wiehe's work [14]. In closed-tube reactors, the distillate product remains in the oil phase resulting in an S_L value more representative of the AS^+ solvation ability of distillates. However, at the lower T of 390°C, both $S_{L,1}$ and $S_{L,2}$ were found to be 0.15. At 390°C, the solubility of MA_d in the N_2 is very low resulting in an oil phase rich in MA_d. This seems to have an influence on the ability of the MA_{vr} and MA^+

to stabilize the AS^{+} in the liquid phase. The use of separate S_L values for MA_{vr} and MA_d in our LR model, was done to specifically capture such an effect. However, there seems to be some cross-influence on the value of $S_{L,1}$ due to the presence of significant amounts of MA_d at lower T. Future work targeted at developing relationships for $S_{L,1}$ and $S_{L,2}$ as functions of MA_{vr} and MA_d concentrations in the liquid phase will help improve the LR model in this aspect.

The values for the rate constant of the maltene core combination reaction (k_3) were found to be almost identical to the rate constant of asphaltene cracking reaction (k_2). This observation was consistent at all three reaction T. A possible explanation for this phenomenon may be that the formation of polynuclear aromatic aryl radicals (the unpaired electron on an aromatic ring C) may be the rate determining step in both these reaction pathways. However, detailed investigations on the fundamental reaction steps in these pathways are needed to understand why k_3 is close to k_2.

Rate constant variation with temperature consistent with Arrhenius rate law

As shown in Fig. 8a to Fig. 8c, the LR rate constants vary with T according to the Arrhenius exponential rate law. The apparent activation energies E_a for k_1 and k_2 based on the Arrhenius best-fit line were 54.9 kcal/mol and 40.4 kcal/mol respectively. As a comparison, the E_a for k_1 and k_2 determined by Wiehe in [14] for the Cold Lake VR thermolysis were 44.3 kcal/mol and 35.3 kcal/mol respectively. These are of similar order to the values calculated in this study providing some support for the goodness of fit for the LR parameters.

3.1.2 Best-fit SCW-phase lumped reaction kinetics parameters

Next, TPSR model simulations of the Shanghai batch reactor VR thermolysis experiments in the presence of SCW were used to infer the LR parameters for the SCW phase using the same procedure described in Section 3.1. In this exercise, the oil-phase kinetics parameters determined in Section 3.1.1 were used as known values. The SCW-phase parameters resulting in the best fit between the TPSR model predictions and the experimental data [3],[4] are given in in Table C2 in the Supplementary Material, along with the corresponding

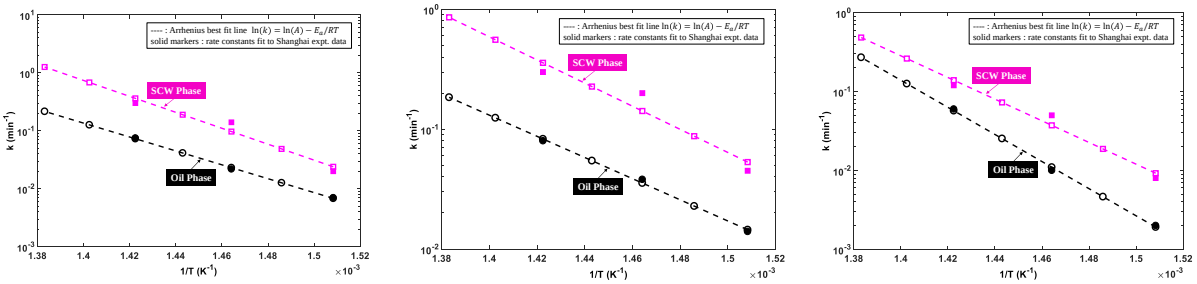

(a) k_1 (b) k_2 (c) k_4

Figure 8: Rate constants for reactions in oil and SCW phases follow the Arrhenius rate law expression $ln(k) = ln(A) - E_a/RT$. The rate constants were fit using the TPSR model to best describe the Shanghai batch reactor experimental data [3],[4]. Here, A and E_a are the apparent pre-exponential factor and activation energy for the reaction respectively.

values for the oil-phase parameters. The TPSR model predictions for the temporal variation of the species lump mass fractions for the best-fit kinetic parameters are shown in Fig. 9a to Fig. 9c along with the experimental data [3],[4] points (solid markers), indicating a good fit between the model predictions and the experimental data. The SCW-phase reaction rate constants broadly follow an Arrhenius exponential variation trend with T as shown in Fig. 8a to Fig. 8c. However, there are significant deviations from the Arrhenius trend-line.

The major differences between the reaction parameters in the oil and SCW phases may be summarized as below:

1. **Significantly faster VR maltene primary cracking in SCW phase:** The ratio of the VR maltene primary cracking reaction (R1) rate constant in the SCW phase to that in the oil phase $k_{1,w}/k_{1,o}$ is $\sim$ 3 to 6 depending on the T, as shown in Table C2 in the Supplementary Material. The VR maltene species have significant amounts of good natural H-donors. They can cause a reduction in the net rate of the thermal cracking free radical chain reaction pathway by terminating the free radicals through H donation. This influence of the presence of natural H-donors in VR feeds on the cracking rate was shown in [48] and [49]. This effect was further verified in those studies by observing experimentally that the addition of an external H-donor like tetralin significantly reduced the cracking rates of VR maltenes and asphaltenes.

   The SCW phase is relatively lean in H-donors as compared to the oil phase as the H-

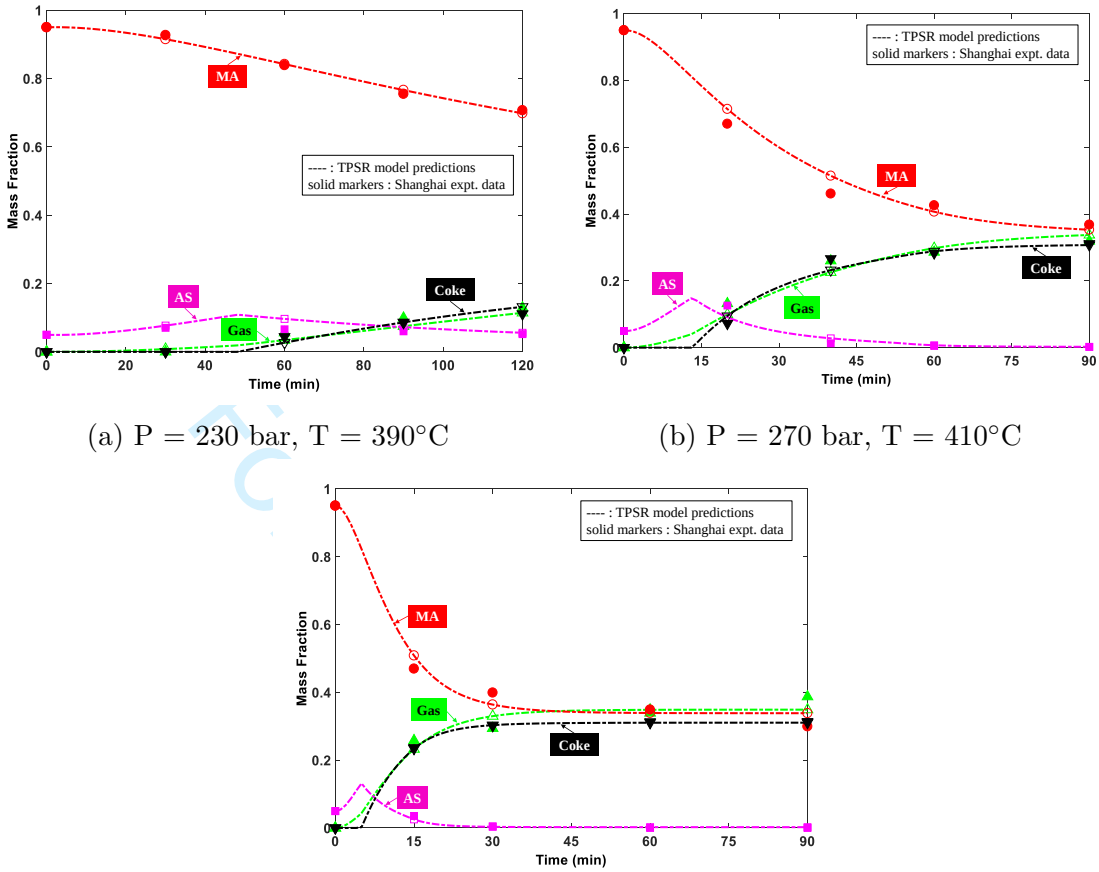

(a) P = 230 bar, T = 390°C

(b) P = 270 bar, T = 410°C

(c) P = 300 bar, T = 430°C

Figure 9: TPSR model predictions of temporal variation of reaction species lumps using the best-fit kinetic parameters for the Shanghai batch reactor experiments ([3],[4]) of VR pyrolysis in the presence of SCW. Nomenclature: MA: total maltene; AS: total asphaltene.

donating maltene species get diluted by the large number of water molecules once they dissolve in the SCW phase. As a result, the free radical chain reaction pathways proceed at higher rates in the SCW phase.

2. **Significantly faster maltene core combination in SCW phase:** The ratio of the maltene core combination reaction (R3) rate constant in the SCW phase to that in the oil phase $k_{3,w}/k_{3,o}$ is ~ 4 to 5 depending on the T, as shown in Table C2 in the Supplementary Material. Thus, the Shanghai experiments do not indicate a suppression of the major coke precursor formation pathway in the SCW phase.
3. **Faster secondary retrograde reactions of distillate maltenes in SCW phase at lower T with the rate enhancement decreasing with T:** The ratio of the distillate

maltene secondary retrograde reaction (R4) rate constant in the SCW phase to that in the oil phase $k_{4,w}/k_{4,o}$ is $\sim$ 4 at lower reaction T of 410°C, as shown in Table C2 in the Supplementary Material. However, this ratio decreases to 2 at 430°C. In addition, at 430°C, the stoichiometric co-efficient for the formation of maltene cores through this reaction (m_1) is lower in the SCW phase ($\sim$ 0.1) as compared to the oil phase ($\sim$ 0.2). The net result is that the rate of formation of MA^+ through reaction (R4) at 430°C is approximately the same in both phases. The difference between $k_{4,w}$ and $k_{4,o}$ continues to decrease with T as seen in Fig. 8c. This points to a possible suppression of the secondary retrograde reaction pathway towards MA^+ in the SCW phase at higher T.

4. **Lower ability of maltenes to stabilize asphaltene cores in SCW phase:** The value of $S_{L,2}$ in the SCW phase is an order of magnitude lower than that in the oil phase as shown in Table C2 in the Supplementary Material. This reflects a drastically reduced ability of the MA_d species to stabilize the AS^+ in the SCW phase. This could result in an earlier onset of coke formation as AS^+ accumulate in the SCW phase through reaction (R3) which is much faster in the SCW phase as shown before.

3.2 Japanese heavy oil thermolysis experiments

Here, the TPSR model was applied to simulate the series of heavy oil thermolysis experiments [5],[6] performed in Japan in a 50 mL stirred autoclave reactor. These works report experimental runs at four different reaction temperatures (420°C, 430°C, 440°C and 450°C) for the thermolysis of a Canadian oil sands bitumen feed containing 47 wt% distillate maltenes, 41.3 wt% vacuum residue maltenes and 11.7 wt% asphaltenes. The operating conditions for these experiments are shown in Table B2 in the Supplementary Material.

In the Japanese experiments, the reaction products were separated into the following fractions and quantified: (i) distillate ($T_b < 525$°C) (ii) vacuum residue ($T_b > 525$°C) (iii) Gas, and (iv) Coke. The mass fraction of asphaltenes was quantified only in the reactant heavy oil feed. The total distillates was determined from the TPSR simulations as the sum of the MA_d, $MA_d{}^{nr}$ and MA^+ species lumps. The pseudo-components used for the

modeling of the feed oil fractions, products and intermediate species are given in Table 3 in the Supplementary Material along with their mass fractions in the initial heavy oil feed.

3.2.1 Best-fit oil-phase and SCW-phase lumped reaction parameters

As in Section 3.1.1, the data from the experimental runs for the heavy oil thermolysis in the presence of N_2 were used to infer the oil-phase LR parameters for the feed used in the Japanese experiments using TPSR model simulations. The SCW-phase LR parameters were then inferred from TPSR model simulations of the experiments in the presence of SCW as described in Section 3.1.2 using the oil-phase parameters obtained earlier. The oil-phase and SCW-phase LR parameters resulting in the best fit between the TPSR model predictions and the experimental data [5],[6] are given in Table C3 in the Supplementary Material. The TPSR model predictions for the temporal variation of the species lump mass fractions for the best-fit kinetic parameters are shown in (i) Fig. 10a to Fig. 10d for the reaction in the presence of N_2, and (ii) Fig. 12a to Fig. 12d for the reaction in the presence of SCW, along with the experimental data [5],[6] points (solid markers). A reasonably good fit was obtained between the model predictions and the experimental data. In particular, the important feature of the coke induction period is captured well.

Similar to the case for the Shanghai VR experiments, the reaction rate constants k_2 and k_3 were found to be very close to each other at all T conditions for both the oil and SCW-phase reactions. The rate constants k_1, k_2 and k_4 for both phases follow an Arrhenius exponential variation with T as shown in Fig. 11a to Fig. 11c. In fact, the goodness-of-fit for the Arrhenius trend-line is even better than in the case of the rate constants for the Shanghai experiments.

The major differences between the oil-phase LR parameters for the heavy oil bitumen in the Japanese experiments and those for the Shanghai VR may be summarized as below:

1. The rate constants for the reactions (R1) to (R4) are lower than those for the Shanghai VR by a factor of 2.5 to 5, with this reactivity factor increasing with T. Here, the Shanghai LR rate constants at T = 390°C, 410°C and 430°C were interpolated and extrapolated to

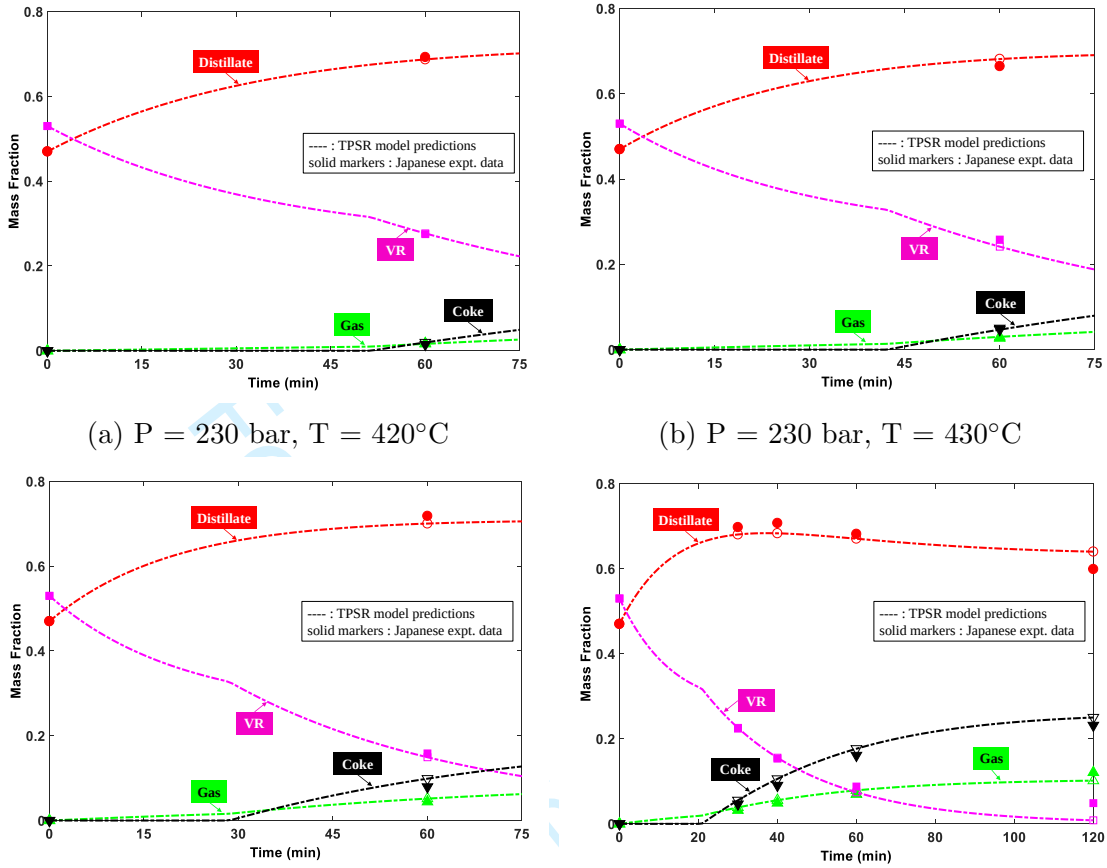

(a) P = 230 bar, T = 420°C (b) P = 230 bar, T = 430°C

(c) P = 240 bar, T = 440°C (d) P = 250 bar, T = 450°C

Figure 10: TPSR model predictions of temporal variation of species lumps using the best-fit kinetic parameters for the Japanese batch reactor experiments ([5],[6]) of heavy oil pyrolysis in the presence of N_2. Nomenclature: Distillate: oil fraction with $T_b < 525$°C; VR: vacuum residue fraction with $T_b > 525$°C.

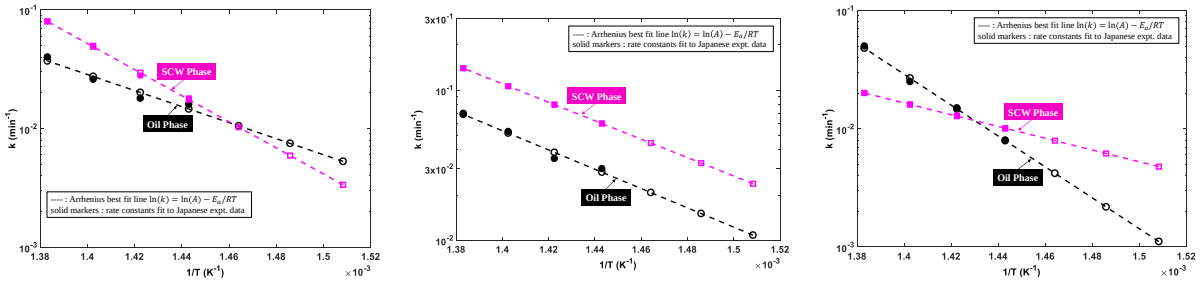

(a) k_1 (b) k_2 (c) k_4

Figure 11: Rate constants for reactions in oil and SCW phases follow the Arrhenius rate law expression $ln(k) = ln(A) - E_a/RT$. The rate constants were fit using the TPSR model to best describe the Japanese batch reactor experimental data [5],[6]. Here, A and E_a are the apparent pre-exponential factor and activation energy for the reaction respectively.

the T conditions of the Japanese experiments (T = 420 to 450 °C) using the Arrhenius exponential rate law as shown in Fig. 8a to Fig. 8c. The lower reactivity of the heavy oil bitumen feed may be explained by the large amount of distillate (47 wt%) in the reactant feed. Most of this distillate fraction ($\sim$ 25 to 30 wt%) is in the heavy gas oils and vacuum gas oils range (425°C $< T_b <$ 525°C). These gas oils are good H-donors rich in multi-ring hydroaromatics (aromatics rings with attached naphthenic rings like in Fig. 6b) as shown by the structural modeling of these bitumen oil fractions in [47]. The abundance of H-donors in the reactant feed leads to the significant reduction in the effective rates of the free radical chain reaction pathways due to free-radical termination induced by the H-donors. In fact, the primary cracking rate constants k_1 and k_2 are lower by a factor of 2.5 to 5 than even the values for Cold Lake VR reported in Wiehe's work [14]. Considering that both the bitumen used in the Japanese experiments and the Cold Lake VR are of Canadian origin, the lower reactivity of whole bitumen is likely to be due to the presence of the vacuum gas oils rather than inherent lower reactivity of the vacuum residue species themselves.

2. As compared to the Shanghai VR feed, the heavy oil bitumen feed has a lower tendency to form maltene cores through the secondary retrograde reaction step as indicated by the values of the stoichiometric co-efficient m_1 in Table C3 in the Supplementary Material.
3. As compared to the Shanghai VR feed, the heavy oil bitumen has a significantly lower tendency to form gas through the secondary cracking of MA_d as reflected in the values of the stoichiometric co-efficient g_1 in Table C3 in the Supplementary Material.

The major differences between the SCW-phase LR parameters for the heavy oil bitumen in the Japanese experiments and those for the Shanghai VR may be summarized as below:

1. **Mild enhancement in VR maltene primary cracking rate constant:** The ratio $k_{1,w}/k_{1,o}$ is close to 1 at 420 °C and increases to 2 at 450 °C, as shown in Table C3 in the Supplementary Material. In contrast, this ratio was $\sim$ 3 to 6 for the Shanghai VR. Thus, there is only a mild enhancement in the primary cracking rate in the SCW phase for the

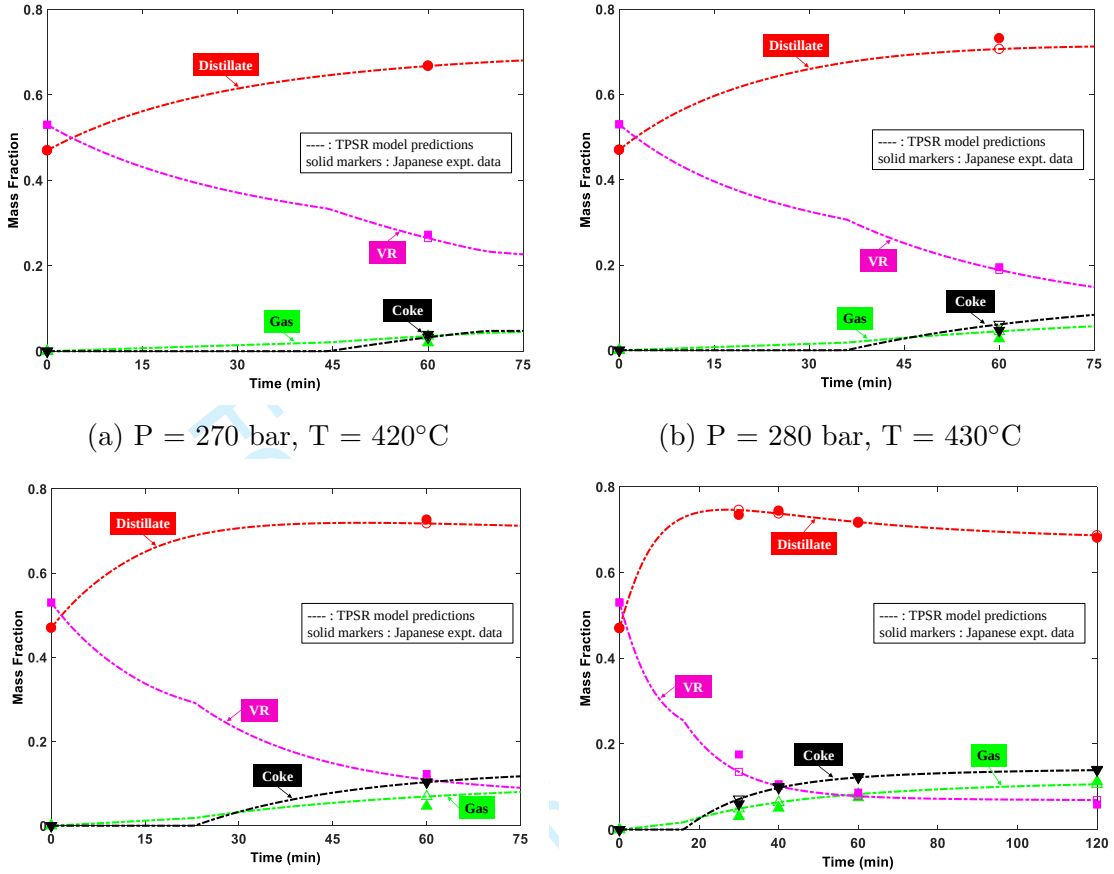

(a) P = 270 bar, T = 420°C (b) P = 280 bar, T = 430°C

(c) P = 290 bar, T = 440°C (d) P = 300 bar, T = 450°C

Figure 12: TPSR model predictions of temporal variation of reaction species lumps using the best-fit kinetic parameters for the Japanese batch reactor experiments ([5],[6]) of heavy oil pyrolysis in the presence of SCW. Nomenclature: Distillate: oil fraction with $T_b < 525$°C; *VR*: vacuum residue fraction with $T_b > 525$°C.

heavy oil bitumen used in the Japanese experiments. As discussed before, the presence of large amounts of H-donating heavy gas oils in the reactant feed significantly lowers the rates of the free-radical chain reaction pathways. These heavy gas oils have significant solubility in the SCW phase at the T, P conditions of the experiments. Consequently, the SCW phase is not as lean in H-donors as in the Shanghai experiments, resulting in only a modest enhancement of the cracking rates.

2. **Suppression of secondary coke formation pathway:** A clear suppression of coke formation was observed in the presence of SCW as compared to the N_2 experiments especially at higher T and longer reaction times as can be seen by comparing Fig. 10d

and Fig. 12d. The inferred LR parameters help isolate the exact cause of this coke suppression effect.

The MA^+ combination reaction (R3) is the primary route towards the formation of extrinsic coke precursors. This reaction is close to 2x faster in the SCW phase as indicated by the k_3 values in Table C3 in the Supplementary Material. Thus, the lower coke formation observed is not due to the suppression of the primary coke precursor formation pathway. The lower coke formation is mainly a result of lower rates of the secondary retrograde reaction (R4) of MA_d in the SCW phase. The ratio $k_{4,w}/k_{4,o}$ decreases from 1.1 to 0.4 with an increase in T from 420°C to 450°C. The stoichiometric co-efficient m_1 for MA^+ formation through reaction (R4) is also lower in the SCW phase ($m_{1,w} = 0.05$) as opposed to the oil phase ($m_{1,o} = 0.1$ - 0.15). Therefore, it is mainly the formation of smaller 2-5 ring polynuclear aromatics or maltene cores from the distillate maltene product that is suppressed in the SCW medium. This is consistent with the observation that reaction in SCW medium results in lower coke formation in studies of model compounds like hexyl-benzene and hexyl-sulfide as reported in [15].

In conclusion, while SCW can deter the formation of smaller PNAs from low-boiling HC species, it may not be effective in preventing the combination of pre-existing smaller PNAs towards coke precursors.

3. **Ability of distillate species to stabilize asphaltene cores in liquid phase is retained in the SCW phase:** Lower solid coke formation at longer reaction times in the presence of SCW is further aided by the retention of the ability of the distillate species in the SCW phase to hold the asphaltene cores in solution. The AS^+ solubility limit co-efficient for MA_d ($S_{L,1}$) in the SCW phase is equal to that in the oil phase as shown in Table C3 in the Supplementary Material. This may be caused by the presence of large amounts of vacuum gas oils as part of the MA_d species in the SCW phase. These are rich in 2 to 4 ring PNAs which are good solvents for larger PNAs or AS^+. In contrast, the $S_{L,1,w}$ value was significantly lower (~ 0.01) for the Shanghai experiments as most of the

distillates in the SCW phase were probably lighter and less aromatic product distillates which are not good solvents for AS^{+}.

4 Conversion to distillates before onset of coke formation

A practical analog of heavy oil upgrading in batch reactors would be the continuous flow of heavy oil or VR through a tubular reactor maintained at high temperature with the feed spending a fixed residence time in the reactor tube. A similar process with co-flow of oil feed and SCW could also be devised to affect upgrading in the presence of SCW. In both of these practical reactor configurations, the residence time will have to be limited to the coke induction period for the feed at the target reactor temperature. Any further reaction would cause solid coke formation in the tube rendering the reactor nonoperational. Hence, an appropriate performance measure for the upgrading process is the conversion to high-value distillate liquids before the onset of coke formation, denoted by $Conv_{dist.}$ $(t{=}t_{Ck=0})$. The $Conv_{dist.}$ $(t{=}t_{Ck=0})$ cannot be trivially estimated from the Shanghai batch reactor experimental data due to (i) measurements at discrete time points resulting in an inability to directly calculate $t_{Ck=0}$ and (ii) measurement of total maltene fraction without differentiation between distillate boiling range liquids and unreacted feed maltenes.

On the other hand, the TPSR model predictions of the Shanghai batch reactor experimental runs have all the detailed information necessary to calculate $Conv_{dist.}$ $(t{=}t_{Ck=0})$. The calculated values are shown in Table 1 for the thermolysis in the presence of both N_2 and SCW at T = 390°C, 410°C and 430°C. Based on this performance measure, one can conclude that the upgrading of the Shanghai VR in the presence of SCW actually results in an inferior outcome as opposed to pure oil phase thermolysis at these temperatures. Thus, in spite of the superior solvent properties of SCW, a simple batch reactor configuration or tubular co-flow reactor configuration may not yield the best upgrading results for the Shanghai VR and similar feeds. A possible improvement in the form of a SCW up-flow extractive upgrading reactor configuration will be evaluated in detail using the TPSR model in a future study.

Though the distillate product fraction was quantified in the Japanese experiments, the

	T = 390°C	T = 410°C	T = 430°C
Presence of N_2	43.8	48.4	46.5
Presence of SCW	30.1	35.4	38.7

Table 1: Conversion to high-value distillate liquids before the onset of coke formation, $Conv_{dist.}$ (t=$t_{Ck=0}$) for the Shanghai VR upgrading experiments inferred using the TPSR model simulations of the same.

$Conv_{dist.}$ (t=$t_{Ck=0}$) could not be trivially estimated from the experimental data due to the measurements at a small number of discrete time points resulting in an inability to directly calculate $t_{Ck=0}$. The problem is exacerbated at the lower T experiments at 420°C, 430°C and 440°C where data points were available only at longer reaction times, away from the coke induction period. On the other hand, the TPSR model predictions of the Japanese batch reactor experimental runs have all the detailed information necessary to calculate $Conv_{dist.}$ (t=$t_{Ck=0}$). The calculated values are shown in Table 2 for the thermolysis in the presence of both N_2 and SCW at T = 420°C, 430°C, 440°C and 450°C. Based on this performance measure, one can conclude that the upgrading of whole heavy oil bitumen in the presence of SCW can actually yield beneficial results as opposed to pure oil phase thermolysis, especially at higher temperatures. Thus, a combination of high heavy gas oil content in the reactant feed and the use of SCW can be a successful strategy for achieving improved yields in a co-flow upgrading reactor. However, as discussed in Section 3.2.1, the primary pathway towards extrinsic coke formation can't be effectively suppressed by the use of SCW in a batch reactor or a continuous co-flow reactor. In order to more effectively target the suppression of extrinsic coke formation using SCW, a possible improvement in the form of a SCW up-flow extractive upgrading reactor configuration will be evaluated using the TPSR model in a future publication.

5 Conclusion

In this work, we demonstrated the inference of oil and supercritical water (SCW) phase-specific kinetics parameters for a compact but effective lumped reaction model for heavy oil upgrading in the presence of SCW through the development and application of a Two-phase

	T = 420°C	T = 430°C	T = 440°C	T = 450°C
Presence of N_2	38.6	35.5	35.0	35.8
Presence of SCW	33.1	38.8	41.4	48.7

Table 2: Conversion to high-value distillate liquids before the onset of coke formation, $Conv_{dist.}$ (t=$t_{Ck=0}$) for the Japanese heavy oil bitumen upgrading experiments inferred using the TPSR model simulations of the same.

Stirred Reactor (TPSR) simulation tool to batch reactor experiments previously reported in the literature. Considering the wide variety and complexity of heavy oils and vacuum residua from around the world, it is hardly possible to obtain a single set of LR kinetics parameters which can universally describe the reaction kinetics for different heavy oil feeds. However, it was shown that the same form of the LR model can be used repeatably to infer parameters that describe the thermolysis kinetics of different reactant feeds at different T, P conditions and in the presence of different reaction media. The TPSR simulation tool developed in this study may be similarly employed for kinetics parameter inference for other different reactant oil feeds, following the general framework established in this paper.

The TPSR simulations enable us to understand the influence of SCW on major chemical reaction pathways in a way that is not possible by a simple examination of the experimental data reported in the literature. We are able to infer that, though SCW can suppress the formation of newer polynuclear aromatics (PNAs) from distillate range species, it is broadly ineffective in deterring the combination of pre-existing PNA fragments in the reactant feed. By providing the detailed information necessary to appropriately quantify the important performance metric of conversion to high-value distillate liquids before the onset of coke formation, the TPSR simulations help arrive at a clearer conclusion as to whether the use of SCW in the batch reactor led to better product outcomes for each of the reactant feeds and operating conditions reported in the experimental studies [3]-[6].

The clear insight obtained from the inferred parameters that SCW may not be effective in suppressing the primary extrinsic coke formation pathway in a batch reactor or co-flow reactor configuration, motivates us towards devising improved reactor configurations which

better exploit the solvent properties of SCW to achieve this goal. One such reactor configuration is the SCW up-flow extractive upgrading reactor, which has already shown promise in previous experimental studies reported in the literature [7],[50],[51]. Furthermore, the performance quantification of the proposed reactor configuration may be done over a wider range of temperatures than that in the experiments from which the LR parameters were inferred, due to the Arrhenius variation of the rate constants with temperature. Such a quantitative performance characterization of the SCW up-flow extractive upgrading reactor will be the focus of a following publication.

Acknowledgements

The authors gratefully acknowledge the support of Saudi Aramco for funding this study under Contract Number 6600023444. In particular, we would like to thank Dr. Ki-Hyouk Choi and his team at the Saudi Aramco R&D Center for their encouragement, support and feedback. We would also like to thank Prof. William H. Green and Prof. Michael T. Timko for their invaluable inputs, enriching discussions and encouraging words.

REFERENCES

[1] Brunner E, "Fluid mixtures at high pressures IX. Phase separation and critical phenomena in 23 (n-alkane+ water) mixtures." The Journal of Chemical Thermodynamics 1990;22(4):335353.

[2] Brunner E, Thies MC, Schneider GM. " Fluid mixtures at high pressures: Phase behavior and critical phenomena for binary mixtures of water with aromatic hydrocarbons." The Journal of supercritical fluids 2006;39(2):160173.

[3] Tan XC, Liu QK, Zhu DQ, Yuan PQ, Cheng ZM, Yuan WK. "Pyrolysis of heavy oil in the presence of supercritical water: The reaction kinetics in different phases." AIChE Journal 2015;61(3):857866.

[4] Liu QK, Zhu DQ, Tan XC, Yuan PQ, Cheng ZM, Yuan WK, Yang JY, "Lumped reaction kinetic models for pyrolysis of heavy oil in the presence of supercritical water." AIChE Journal 2016;62(1):207216.

[5] Morimoto M, Sugimoto Y, Saotome Y, Sato S, Takanohashi T. "Effect of supercritical water on upgrading reaction of oil sand bitumen." The Journal of Supercritical Fluids 2010;55(1):223231.

[6] Morimoto M, Sugimoto Y, Sato S, Takanohashi T. "Solvent effect of water on supercritical water treatment of heavy oil." Journal of the Japan Petroleum Institute 2014;57(1):1117.

[7] Vilcez J, Watanabe M, Watanabe N, Kishita A, Adschiri T. "Hydrothermal extractive upgrading of bitumen without coke formation." Fuel 2012;102:379385.

[8] Cheng ZM, Ding Y, Zhao LQ, Yuan PQ, Yuan WK. "Effects of supercritical water in vacuum residue upgrading." Energy & Fuels 2009;23(6):31783183.

[9] Li N, Yan B, Xiao XM. "A review of laboratory-scale research on upgrading heavy oil in supercritical water." Energies 2015;8(8):89628989.

[10] Kishita A, Watanabe N, Vilcaez Perez J et al. "Observation of the heavy crude oil dissolution behavior under supercritical condition of water." In: International Petroleum Technology Conference 2009.

[11] Kishita A. "Observation study of the heavy crude oil dissolution behavior under supercritical condition of water." In: International Petroleum Technology Conference, Doha, Qatar, 2009;29212924.

[12] Gudiyella S, Lai L, Borne IH, Tompsett GA, Timko MT, Choi KH, Alabsi MH, Green WH. "An experimental and modeling study of vacuum residue upgrading in supercritical water." AIChE Journal 2018;64(5):17321743.

[13] Wiehe IA. "A phase-separation kinetic model for coke formation." Industrial & Engineering Chemistry Research 1993;32(11):24472454.

[14] Wiehe IA. "Process chemistry of petroleum macromolecules." CRC press; 2008.

[15] Kida Y. "Supercritical water desulfurization of crude oil." PhD thesis, Massachusetts Institute of Technology; 2014.

[16] Levinter ME, Medvedeva MI. Panchenkov GM, Aseev YG, Nedoshivin YN, Finkel'shtein GB, Galiakbarov MF. "Mechanism of coke formation in the cracking of component groups in petroleum residues." Chemistry and Technology of Fuels and Oils 1966;2(9):628632.

[17] Levinter ME, Medvedeva MI. Panchenkov GM, Agapov GI, Galiakbarov MF, Galikeev RK. "The mutual effect of group components during coking." Chemistry and Technology of Fuels and Oils 1967;3(4):246249.

[18] Magaril R, Aksenova E. "Study of mechanism of coke formation in cracking of petroleum resins." International Chemical Engineering 1968;8(4):727.

[19] Valyavin G, Fryazinov V, Gimaev R, Syunyaev Z, Vyatkin YL, Mulyukov SF. "Kinetics and mechanism of the macromolecular part of crude oil." Chemistry and Technology of Fuels and Oils 1979;15(8):562566.

[20] Takatsuka T, Kajiyama R, Hashimoto H, Matsuo I, Miwa S. "A practical model of thermal cracking of residual oil." Journal of Chemical Engineering of Japan 1989;22(3):304310.

[21] Schucker R, Keweshan C. "Reactivity of Cold Lake asphaltenes." Am. Chem. Soc., Div. Fuel Chem., Prepr.; (United States) 1980;25;CONF-800814-P2.

[22] Savage PE, Klein MT, Kukes SG. "Asphaltene reaction pathways. 1. Thermolysis" Industrial & Engineering Chemistry Process Design and Development 1985;24(4):11691174.

[23] Savage PE, Klein MT, Kukes SG. "Asphaltene reaction pathways. 3. Effect of reaction environment." Energy & Fuels 1988;2(5):619628.

[24] Magaril RZ, Aksenova EI. "Investigation of the mechanism of coke formation during thermal decomposition of asphaltenes." Chemistry and Technology of Fuels and Oils 1970;6(7):509512.

[25] Magaril RZ, Ramazaev LF, Aksenova EI. "Kinetics of Formation of Coke in Thermal Processing of Crude Oil." International Chemical Engineering 1971;11(2):250.

[26] Sosnowski J, Turner DW, ENG J. "Upgrading Heavy Crudes to Clean Liquid Products." In: AIChE 88th National Meeting, Philadelphia, 1980.

[27] Takatsuka T, Wada Y, Hirohama S, Fukui Y. "A prediction model for dry sludge formation in residue hydroconversion." Journal of Chemical Engineering of Japan 1989;22(3):298303.

[28] Li N, Yan B, Xiao XM. "Kinetic and reaction pathway of upgrading asphaltene in supercritical water." Chemical Engineering Science 2015;134:230237.

[29] Raghavan A. "Two-phase stirred reactor (TPSR) modeling tool source code repository." `https://github.com/rashwin1989/batch_wsr_kinetic/`, 2018.

[30] Wiehe IA. "A solvent-resid phase diagram for tracking resid conversion." Industrial & Engineering Chemistry Research 1992;31(2):530536.

[31] Michelsen ML. "The isothermal flash problem. Part I. Stability." Fluid Phase Equilibria 1982;9(1):119.

[32] Michelsen ML. "The isothermal flash problem. Part II. Phase-split calculation." Fluid Phase Equilibria 1982;9(1):2140.

[33] Raghavan A. "Numerical simulations of supercritical water-hydrocarbon mixing in a 3-D cylindrical tee mixer." Masters thesis, Massachusetts Institute of Technology, 2014.

[34] Raghavan A, Ghoniem AF. "Simulation of supercritical water–hydrocarbon mixing in a cylindrical tee at intermediate Reynolds number: Formulation, numerical method and laminar mixing." The Journal of Supercritical Fluids 2014;92:3146.

[35] Raghavan A. "Multi-scale modeling tools for coupled reaction, phase equilibrium and two-phase mixing phenomena with application to supercritical water heavy oil upgrading process." PhD thesis, Massachusetts Institute of Technology, 2019.

[36] Peng DY, Robinson DB. "A new two-constant equation of state." Industrial & Engineering Chemistry Fundamentals 1976;15(1):5964.

[37] Robinson DB, Peng DY. "The characterization of the heptanes and heavier fractions for the GPA Peng-Robinson programs." Gas Processors Association, 1978.

[38] Jaubert JN, Mutelet F. "VLE predictions with the Peng-Robinson equation of state and temperature dependent kij calculated through a group contribution method." . Fluid Phase Equilibria 2004;224(2):285304.

[39] Jaubert JN, Vitu S, Mutelet F, Corriou JP. "Extension of the PPR78 model (predictive 1978, Peng-Robinson EOS with temperature dependent kij calculated through a group contribution method) to systems containing aromatic compounds." Fluid Phase Equilibria 2005;237(1-2):193211.

[40] Vitu S, Jaubert JN, Mutelet F. "Extension of the PPR78 model (Predictive 1978, Peng-Robinson EOS with temperature dependent kij calculated through a group contribution method) to systems containing naphtenic compounds." Fluid Phase Equilibria 2006;243(1-2):928.

[41] Qian JW, Privat R, Jaubert JN. "Predicting the phase equilibria, critical phenomena, and mixing enthalpies of binary aqueous systems containing alkanes, cycloalkanes, aromatics, alkenes, and gases (N2, CO2, H2S, H2) with the PPR78 equation of state." Industrial & Engineering Chemistry Research 2013;52(46):1645716490.

[42] Kehiaian HV, Sosnkowska-Kehiaian K, Hryniewicz R. "Enthalpy of mixing of ethers with hydrocarbons at 25°C and its analysis in terms of molecular surface interactions." J Chim Phys 1971;68:922934.

[43] Abdoul W, Rauzy E, Pneloux A. "Group-contribution equation of state for correlating and predicting thermodynamic properties of weakly polar and non-associating mixtures: Binary and multicomponent systems." Fluid Phase Equilibria 1991;68:47102.

[44] NIST. "The NIST Chemistry Webbook." `https://webbook.nist.gov/.`

[45] Yaws CL. "Yaws' Critical Property Data for Chemical Engineers and Chemists." Knovel, 2012.

[46] Lee BI, Kesler MG. "A generalized thermodynamic correlation based on three-parameter corresponding states." AIChE Journal 1975;21(3):510527.

[47] He P, Ghoniem AF. "A group contribution pseudocomponent method for phase equilibrium modeling of mixtures of petroleum fluids and a solvent." Industrial & Engineering Chemistry Research 2015;54(35):88098820.

[48] Gould KA, Wiehe IA. "Natural hydrogen donors in petroleum resids." Energy & Fuels 2007;21(3):11991204.

[49] Liu QK, Xu Y, Tan XC, Yuan PQ, Cheng ZM, Yuan WK. "Pyrolysis of asphaltenes in subcritical and supercritical water: Influence of H-donation from hydrocarbon surroundings." Energy & Fuels 2017;31(4):36203628.

[50] Morimoto M, Sugimoto Y, Sato S, Takanohashi T. "Bitumen cracking in supercritical water upflow." Energy & Fuels 2014;28(2):858861.

[51] Fedyaeva ON, Shatrova AV, Vostrikov AA. "Effect of temperature on bitumen conversion in a supercritical water flow." The Journal of Supercritical Fluids 2014;95:437443.